JOURNAL OF MATERIALS SCIENCE 27 (1992) 990–1000

Basic longitudinal texture and fracturing process in thermoset polymers

J. S. COVAVISARUCH*, R. E. ROBERTSON, F. E. FILISKO†
Department of Materials Science and Engineering, The University of Michigan, Ann Arbor, MI 48109-2136, USA

The "basic longitudinal texture", which is present everywhere on the fracture surfaces of glassy thermosets and is the finest texture observed on such surfaces, consists of low ridges and shallow grooves that are aligned parallel with the direction of crack propagation. The periodicity of the basic longitudinal texture, i.e., the average lateral separation between the ridges (or grooves), has been found to be characteristic of materials. This and other properties were measured for a series of rigid epoxy specimens made from diglycidyl ether of bisphenol-A and methylhexahydrophthalic anhydride. For the series of epoxies studied, the glass transition temperatures varied from 76 to 143 °C, the room temperature Young's modulus varied from 2.29 to 2.97 GPa, the room temperature yield stress in compression varied from 99 to 128 MPa, the room temperature Knoop hardness numbers varied from 133.5 to 163.5, the rubbery modulus at 200 °C varied from 12.8 to 21.6 MPa, and the periodicity of the basic longitudinal texture varied from 205 to 368 nm. Only properties of the liquid state, namely glass transition temperature and the rubbery modulus, correlated well with periodicity of the basic longitudinal texture. This suggests that the basic longitudinal texture is the remnant left on the fracture surfaces of a liquid state that must have developed during fracture. This suggests in turn that liquefaction is an intrinsic part of the brittle fracture of polymer network glasses.

1. Introduction

Irrespective of the method of fracture, the "basic longitudinal texture" is present everywhere on the fracture surfaces of glassy thermosets [1–3] and may be present on the fracture surfaces of all network glasses, inorganic as well as organic [4]. The basic longitudinal texture (BLT) is the finest texture observed on such surfaces. It consists of low ridges and shallow grooves that are aligned parallel with the direction of crack propagation. An example is shown in Fig. 1. The BLT has been hypothesized to arise from the unstable growth of the crack at a quasi-air–liquid interface that tends to develop into a pattern of parallel fingers reaching ahead of the crack. This "crack fingering hypothesis" is shown in Fig. 2 [1, 3]. The hypothesis is based on an analogy with the meniscus instability that can develop between two immiscible fluids when accelerated [5]. A similar process was suggested for the crazing of thermoplastics by Argon and Salama [6] and confirmed experimentally by Donald and Kramer [7]. According to the hypothesis, the network glass would be transformed by the fracturing process into a liquid, or at least into a state with liquid-like fluidity, and the BLT is the frozen remnant of this state. The purpose of the work described herein was to test this hypothesis.

The periodicity of the BLT (i.e., the lateral separation between adjacent ridges or grooves) was found in the course of this work to be characteristic of the material rather than of the fracturing process. This is indicated in Fig. 3, which is a micrograph of the fracture surfaces of a specimen obtained by fracturing with a single crack a pair of materials that had been joined together before fracturing [8]. The pair of materials was made from the same amine-cured epoxy except that the one on the left had been aged at 200 °C for 8 h after curing before the epoxy on the right had been applied and cured in-place. As the crack passed from the aged epoxy on the left to the unaged epoxy on the right, the periodicity of the BLT is seen to have enlarged immediately – in a distance smaller than the periodicity or lateral separation between ridges. Being a material property, then, the periodicity of the BLT has been measured for a series of anhydride-cured epoxies and is compared with other properties of these materials.

2. Experimental procedure

2.1. Materials

A series of epoxy plaques was prepared from Dow Chemical Company's general purpose D.E.R. 331 bifunctional liquid diglycidyl ether of bisphenol-A (DGEBA) epoxy resin. This resin was cured with a liquid cyclic anhydride curing agent, methylhexahydrophthalic anhydride (MHHPA). The

* *Present address*: Department of Chemical Engineering, Faculty of Engineering, Chulalongkorn University, Bangkok, BK 10500, Thailand.
† Author to whom correspondence should be addressed.

0022–2461

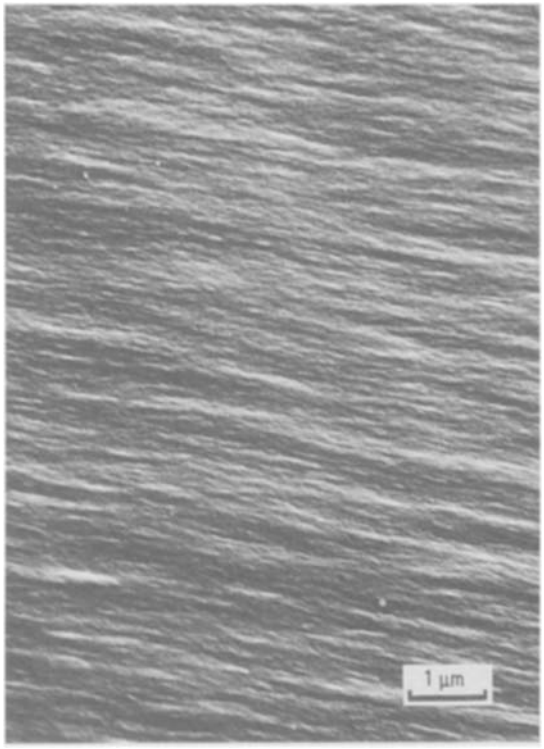

Figure 1 The basic longitudinal texture on an epoxy fracture surface, consisting of low intermittent ridges and shallow grooves aligned in the crack propagation direction.

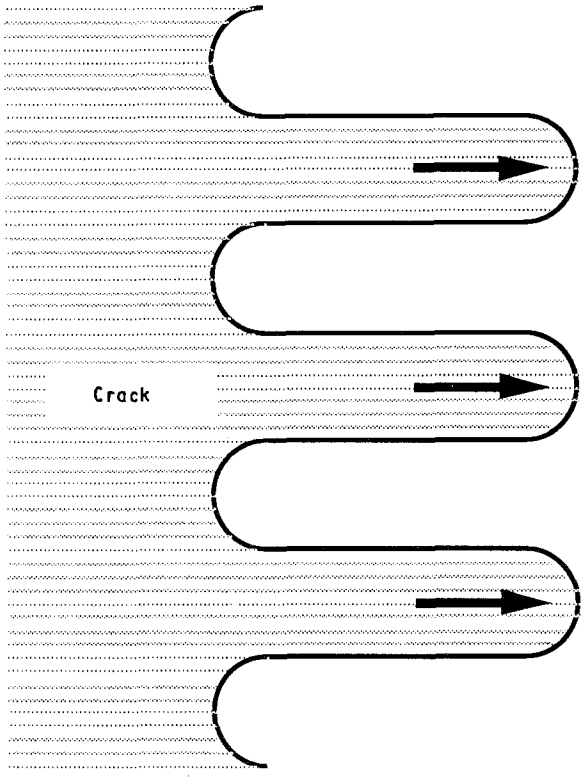

Figure 2 Crack fingering hypothesis.

anhydride was obtained from both Ftalital (Germany) and from Shin-Nippon Rica (Japan). It was employed at concentrations above and below stoichiometry. A tertiary amine, N,N-dimethylbenzylamine (Aldrich Chemical Company), was added as an accelerator.

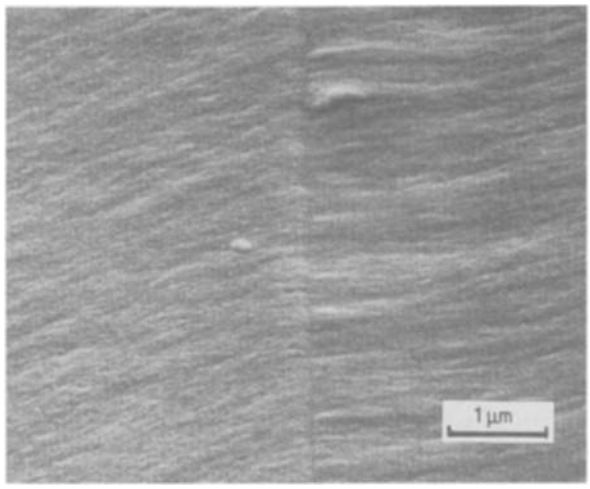

Figure 3 The basic longitudinal texture on the fracture surfaces of aged and unaged amine-cured bisphenol A epoxy that had been bonded and fractured by a single crack.

TABLE I Epoxy formulations and cure conditions

MHHPA hardener[a] (phr)	Accelerator[b] (wt %)	Temperature (°C)	
		Cure (2 h)	Postcure (6 h)
44	2	80°	150°
111	2	80°	150°
44	1	80°	150°
111	1	80°	150°
44	2	120°	150°
111	2	120°	150°
44	1	120°	150°
111	1	120°	150°

[a] The amount at stoichiometry is 88 phr.
[b] N,N-dimethylbenzylamine.

The formulations and cure conditions for the specific specimens studied are given in Table I.

Each formulation was prepared and mixed while it was warmed on a hot plate to 50 ± 5 °C. The mixture was then degassed and moulded into plaques in a closed Teflon-coated mould that was placed vertically in an air circulating oven set at the desired cure and postcure temperatures. The dimensions of the plaques were $203 \times 203 \times 6$ mm^3. All specimens were oven-cooled to room temperature after postcure.

2.2. Fractography

The epoxy resins were fractured in mode I cleavage by three-point bending and double torsion. The first was conducted at three temperatures: room temperature, a temperature close to the boiling point of liquid nitrogen (− 180 °C), and 60 °C. Fracture by double torsion was performed at room temperature only.

Specimens for fracturing in three-point bending were of the size $40 \times 10 \times 6$ mm^3. To initiate fracture, each specimen was scratched with a razor blade along the middle of the underside across the 10 mm dimension. For fracturing at a temperature close to the boiling point of liquid nitrogen (− 180 °C), the specimen was immersed in liquid nitrogen, kept there until

the bubbling caused by the immersion diminished, removed, and quickly fractured. The 60 °C fracture was performed in a heated chamber mounted on an Instron testing machine.

Specimens for fracturing in double torsion were of the size $40 \times 80 \times 6$ mm^3. Into these was machined a U-shaped groove 1 mm in width and 3 mm in depth running the length of the specimen in the centre of the 40 mm dimension, to guide the propagating crack. To initiate the crack, an edge notch was slit on one end of the specimen with a diamond saw, and then a sharp crack 22 to 25 mm long was initiated by forcing a chilled razor blade through the slit. This length for the initial crack was based on the theoretical study of stresses in the specimen. From a three-dimensional elastic finite element stress analysis, the stress intensity was found to be nearly constant when the crack length was greater than about 55% of the specimen width and the remaining ligament length of the specimen for the crack to propagate through was greater than about 65% of the specimen width [9]. The test was carried out at a constant crosshead speed of 0.05 mm min^{-1} or 0.002 in min^{-1} on the Instron mechanical testing machine.

For fractography, the fracture surfaces were cleaned by blowing on them with a compressed gas to dislodge any adhering loose particles. The non-conductive epoxy surfaces were then coated with carbon or gold/palladium. At a plasma discharge current of 10 mA, a voltage of 7 V, argon as the discharge gas, and an exposure time of 3 min, the Au–Pd coating deposited was approximately 35 nm thick. The coated fracture surfaces were examined by scanning electron microscopy at accelerating voltages of 5 and 10 kV. The specimen normal was often tilted toward the secondary electron detector to enhance the contrast of the relatively fine basic longitudinal texture. Stereographic images, obtained by the tilting technique, were used for three-dimensional studies of the fractographic detail.

The average periodicity, the spacing between the peaks of adjacent ridges in the basic longitudinal texture, was measured either from individual or from stereo fractographs at high magnification. The measurement was carried out by aligning the legs of a pair of calipers with the more persistent and reasonably long ridges. At high magnification, some short and extremely fine ridges became visible between the prominent and persistent ones. Due to their lack of either continuity or persistence or both, these extremely fine ridges were not regarded as the basic longitudinal texture. In this experiment, 24 to 30 measurements were made at various locations on fractographs taken at a magnification of 10000×.

2.3. Mechanical properties

The elastic, pre-yielding, and yielding behaviour at room temperature was studied by uniaxial compression. Small rectangular specimens were compressed between two polished tungsten carbide plates mounted on an Instron mechanical testing machine. The dimensions of the specimens were $10 \times 12 \times 3$ mm^3. To reduce the frictional constraint on the specimen, molybdenum disulphide was applied between the plates and the specimen. The constant crosshead speed was 1.3 mm min^{-1} or 0.05 in min^{-1}. The compressive load and corresponding displacement were recorded continuously on a chart and then converted for use to engineering stress and strain.

The dynamic mechanical behaviour was measured at a frequency of 0.32 Hz with a DuPont 983 Dynamic Mechanical Analyzer (DMA). The specimens were investigated over a temperature range from room temperature to 250 °C at a heating rate of 5 °C min^{-1}. The specimens of dimensions $10 \times 40 \times 2$ mm^3 were prepared by cutting with a diamond saw. Each was then dried in a vacuum oven for 24 h before being mounted vertically between a pair of serrated clamps inside the DMA temperature-control chamber. The serrated clamps were preferred because the epoxies were subjected to drastic changes in modulus and hardness over the broad testing temperature range. The torque applied to the clamp screws to hold the specimen was kept constant at 7 in lb. Each specimen was calibrated and measured for corresponding length correction as well as the Young's modulus at resonance. All calibrations were performed at room temperature.

The microhardness was measured with a Tukon Microhardness tester. Specimens were prepared by cutting two parallel surfaces that were then ground and polished on 600, 800 and 1200 grit wheels, sequentially. The samples were tested under a load of 1 kg with an 1/16 in, diamond tip indentor. The indentations were measured in filar count and converted to the actual length of indentation and the Knoop Hardness Number (KHN).

2.4. Thermal properties

The glass transition temperature was measured by using a Mettler TMA 40 thermomechanical analyser (TMA). Specimens were prepared by cutting two parallel surfaces to give a thickness of 2 mm. The specimen thickness was measured prior to heating. This was achieved by placing one of the parallel surfaces on the sample support beneath the calibrated and zeroed pointed probe of the TMA. To maintain contact between the probe and specimen, a small force of 2.5 mN was applied through a 1 mm^2 quartz pointed probe. The heating rate was constant at 5 °C min^{-1}. To eliminate indentation that could have been caused by the pointed probe, an alumina oxide disc of 6 mm diameter was placed between the probe and the specimen. Each specimen was tested a number of times at various locations on the surface. The glass transition temperature was taken as the temperature at which the change in the linear expansion coefficient was most abrupt.

3. Results

3.1. Periodicity of the basic longitudinal texture

As has been mentioned, the basic longitudinal texture is observed over the entire fracture surface irrespective

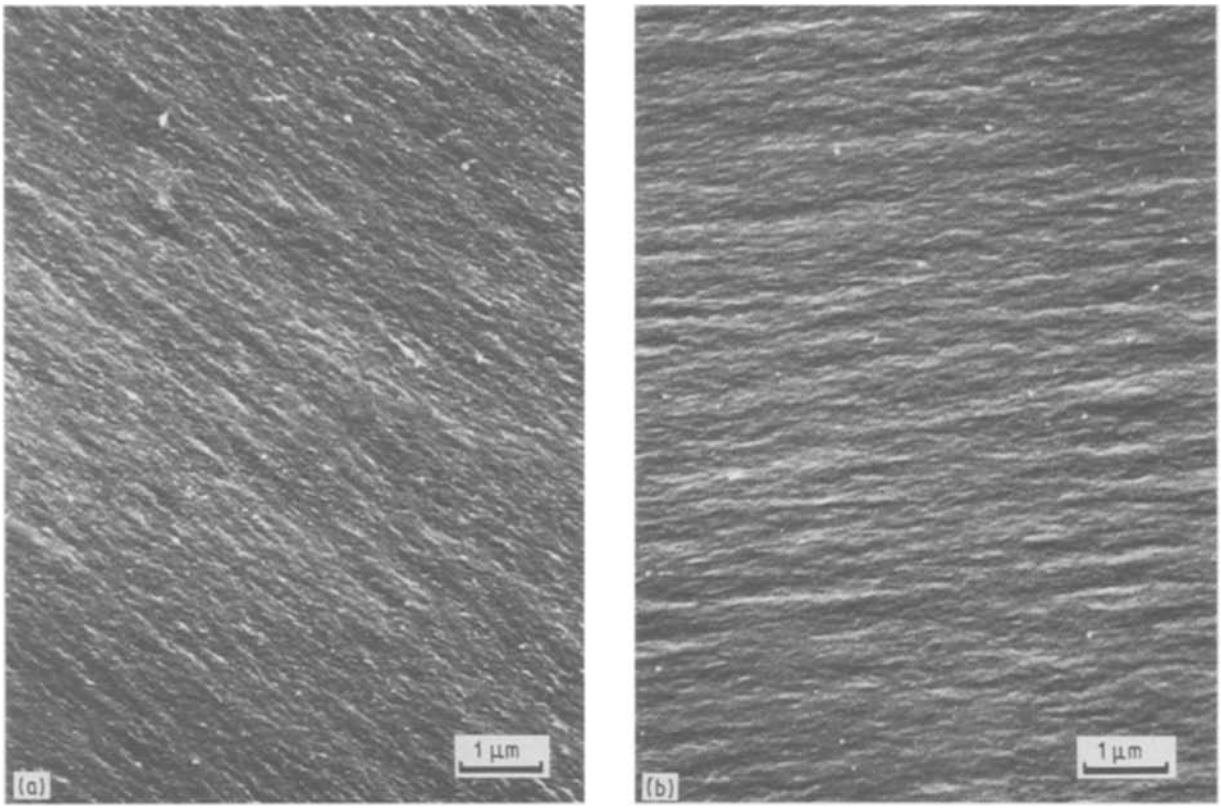

Figure 4 Basic longitudinal texture on epoxy surfaces fractured at (a) approximately − 180 °C and (b) 60 °C.

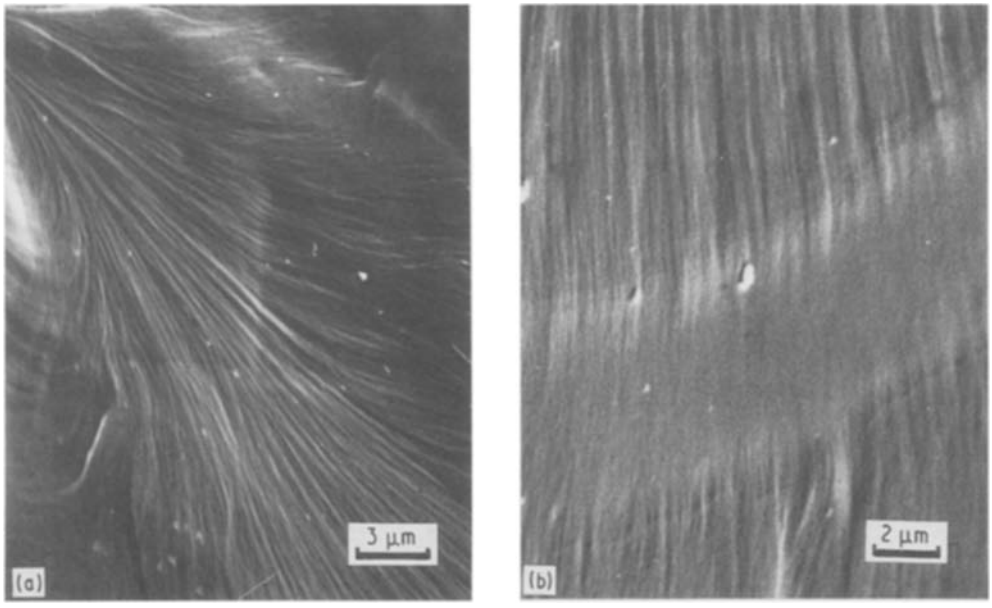

Figure 5 Basic longitudinal texture on epoxy surfaces (a) just beyond a site of crack initiation and (b) at a crack arrest band.

of the fracture conditions: the fracturing method, the temperature, or the crack speed. As is evident from Fig. 4a, the basic longitudinal texture was present in abundance even as the fracturing temperature approached that of liquid nitrogen, − 180 °C. Moreover, when the fracturing temperature was changed from about − 180 to 60 °C (Fig. 4b), the general nature of the basic longitudinal texture was not altered. Similarly, the basic longitudinal texture for high speed fracture (Fig. 5a) is similar to that at the site of crack arrest–initiation (Fig. 5b), where the crack comes to a momentary stop. (Although the BLT seems to disappear in the centre of the arrest–initiation band, it has just become too faint to be visible in this micrograph.) The composition and cure conditions of the thermoset, however, do change the BLT, as seen in Fig. 6, where two epoxy specimens differing in the amount of anhydride curing agents are compared. The BLT of the epoxy with the lower concentration of curing agent appears rougher, with larger amplitudes for the ridges and grooves. With higher concentration of curing agent, the fracture surfaces appear smoother.

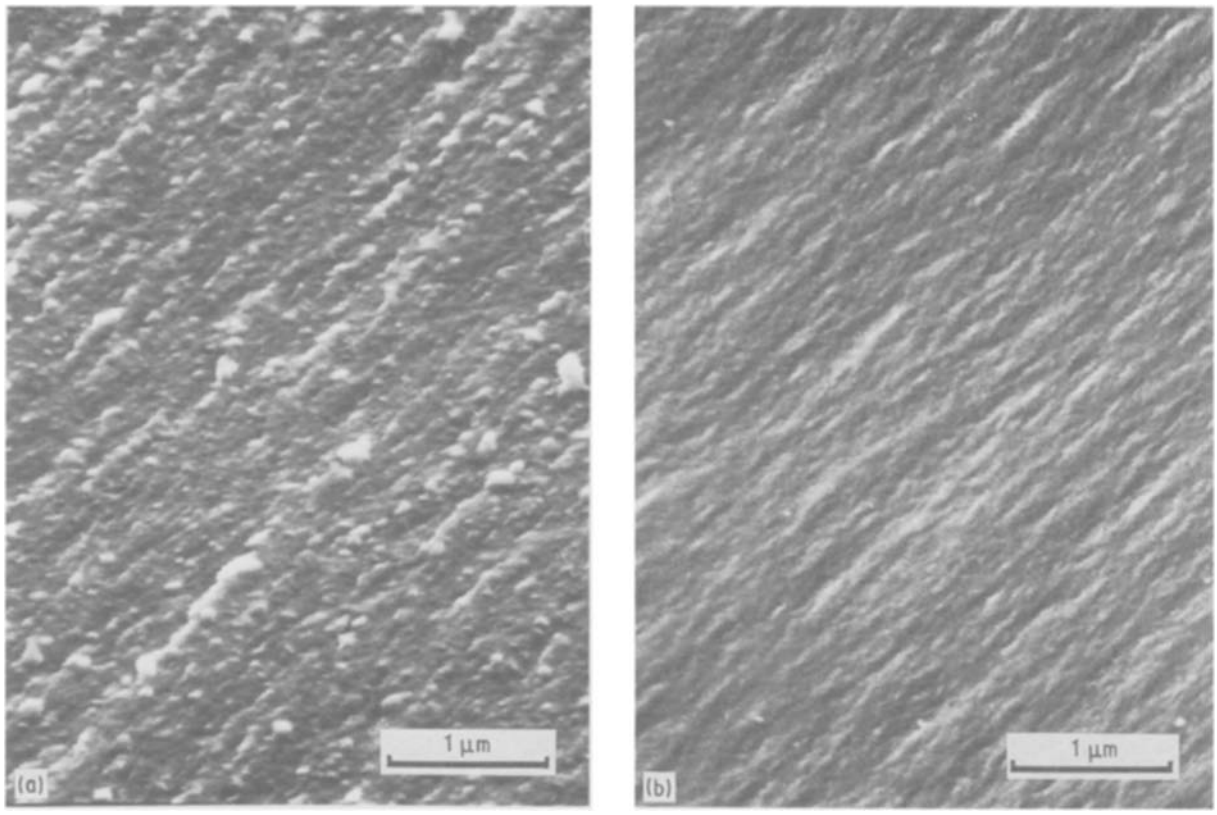

Figure 6 Basic longitudinal texture for epoxy resin cured with (a) 44 phr and (b) 111 phr of anhydride.

TABLE II Glass transition temperature, periodicity of the basic longitudinal texture, and average molecular weight between crosslinks

MHHPA (phr)	Accelerator[a] (wt %)	Cure[b] (°C)	Periodicity at 20°C (nm)	T_g (°C)	M_c
44	1	120	368	75.9	1109
44	1	80	306	90.0	–
44	2	120	296	103.5	896
44	2	80	262	121.6	–
111	2	120	220	131.8	748
111	1	120	212	136.0	687
111	2	80	210	137.1	772
111	1	80	205	142.5	656

[a] N,N-dimethylbenzylamine, % based on weight of epoxy and anhydride.
[b] Cured for 2 h at temperature indicated and postcured for 6 h at 150 °C.

As seen in Figs 1, 4, 5, and 6, there exists a distinct periodicity of the basic longitudinal texture in the direction perpendicular to the ridges and grooves (i.e. perpendicular to the direction of crack propagation). The average periodicity for fracture at 20 °C for each of the epoxy systems studied is tabulated in Table II. The periodicities found ranged from 205 to 368 nm, being finer for the epoxies with less concentration of anhydride. In contrast to the prominent lateral periodicity, the lengths of the ridges in the basic longitudinal texture lay in a much broader range, varying by an order of magnitude. Most of the ridges were between about 820 to 1900 nm long.

3.2. Periodicity of the BLT as opposed to other material properties

The periodicity of the BLT can be compared with the mechanical properties of these materials. The elastic moduli at room temperature measured in uniaxial compression are listed in Table III. There is little variation in the room temperature Young's moduli among these specimens, though there may be a slight increase with crosslink density. When compared with the periodicity of the basic longitudinal texture, as is done in Fig. 7, there is seen to be no statistically significant interdependence between the Young's modulus of these specimens and the periodicity.

To be able to compare the BLT periodicity with the non-linear behaviour of the specimens just before yield, these regions of the compression stress–strain curves were fitted to the following power-law equation [10–12]

$$\sigma = K\varepsilon_i^n \quad (1)$$

where σ is the stress, K and n fitting constants, and ε_i

TABLE III Periodicity of the basic longitudinal texture, Young's modulus, yield stress, yield strain, Knoop hardness, and 1 s flexural modulus in the rubbery plateau at 200 °C

Periodicity (nm)	Young's modulus (GPa)	Yield stress (MPa)	Yield strain (%)	Knoop hardness KHN	1 s Modulus at 200 °C (MPa)
368	2.29	99	0.063	133.5	12.8
306	2.73	116	0.063	139.5	–
296	2.59	107	0.066	134.0	15.8
262	2.42	105	0.069	135.5	–
220	2.92	128	0.065	163.5	18.9
212	2.31	110	0.072	133.5	20.6
210	2.97	127	0.070	149.5	18.3
205	2.81	121	0.066	145.0	21.6

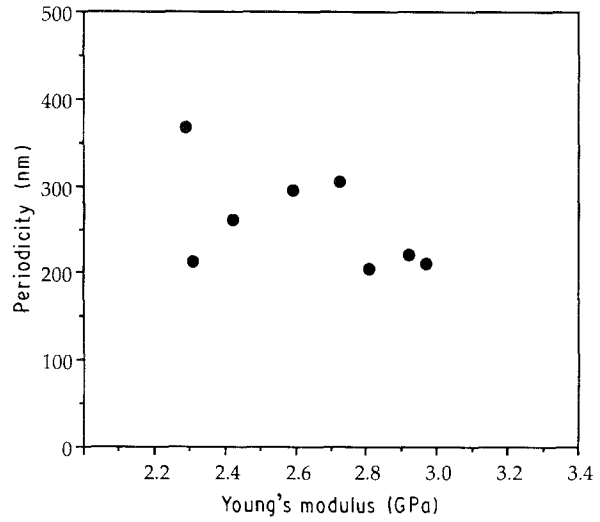

Figure 7 Comparison between the periodicity of the basic longitudinal texture and the Young's modulus.

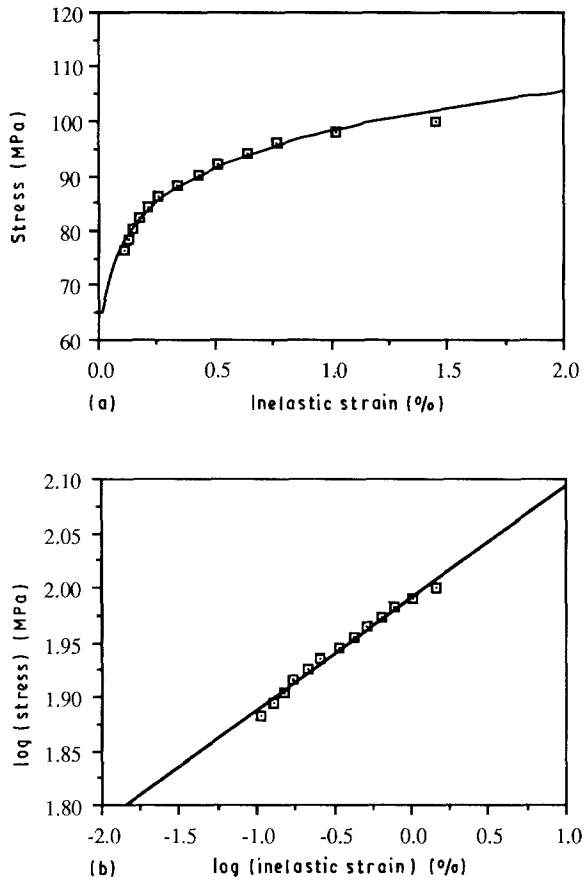

Figure 8 Comparison between the measured stress and the strain in the pre-yield region (points) and the power-law equation (solid line): (a) linear stress plotted against linear inelastic strain, (b) log(stress) plotted against log (inelastic strain).

the inelastic strain (the total strain minus the elastic strain). Fig. 8 demonstrates the quality of fit obtainable between this power-law equation and the engineering stress–strain curves from the pre-yield region of the compression test. The power-law coefficient (K) was found to vary for the specimens studied from 99.7 to 132.4 MPa; the power-law exponent, n, was found to vary from 0.110 to 0.141. These fitting parameters are compared with the periodicity of the basic longitudinal texture in Figs 9 and 10. There is seen to be essentially no correlation between either the coefficient K or the exponent n and the periodicity. In addition to the near random correspondence, both K and n remain relatively unchanged while the periodicity nearly doubles.

The periodicity can be compared also with the yield behaviour. The yield stresses and yield strains also obtained from the compression test are given in Table III. Yielding tends to occur at higher stresses in the specimens containing larger amounts of curing agent. The yield stress, σ_y, varied over the range from 99 to 127 MPa; the yield strain, ε_y, varied over the narrow range from 6.3 to 7.2%. The comparisons between the periodicity of the BLT and the yield stress and the yield strain are given in Figs 11 and 12, respectively. The periodicity is seen to be only weakly related to either the yield stress or the yield strain.

The hardness is a measure of some combination of the elastic modulus and the yield strength. Knoop hardness numbers (KHN) for the series of epoxies studied was found to range from 133.5 to 163.5. These are compared with the periodicity of the BLT in Fig. 13. Since the periodicity was uncorrelated with the Young's modulus and only weakly correlated with the yield stress, it is not surprising that there is little correlation between the periodicity and the Knoop hardness numbers.

The glass transition temperatures obtained for the epoxy specimens from the TMA measurements are listed in Table II. The glass transition temperatures (T_gs) obtained span a fairly large range of 70 °C. Specimens made with lesser amounts of cross-linking agent (44 phr) possessed lower T_gs, ranging from 73 °C

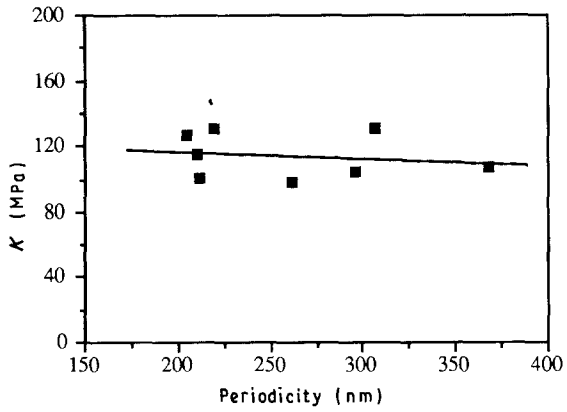

Figure 9 Comparison between the power-law equation coefficient K for pre-yielding and the periodicity of the basic longitudinal texture.

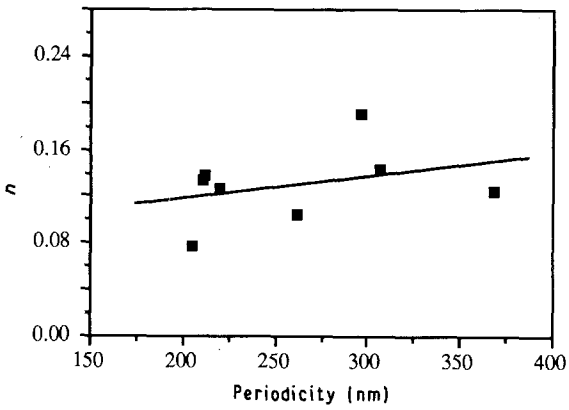

Figure 10 Comparison between the power-law equation exponent n for pre-yielding and the periodicity of the basic longitudinal texture.

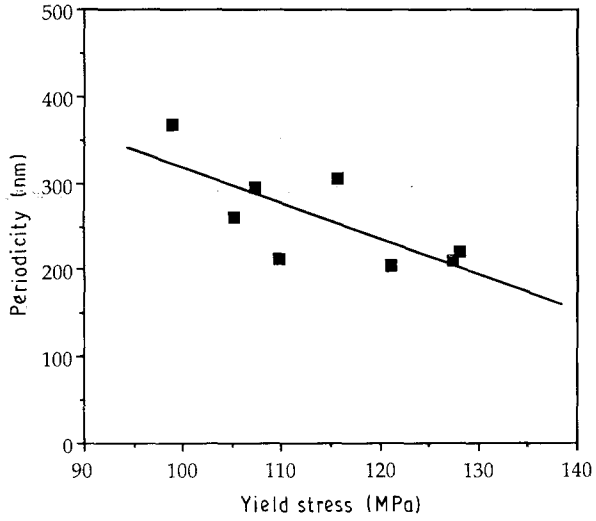

Figure 11 Comparison between the periodicity of the basic longitudinal texture and the yield stress.

(346 K) to 121.6 °C (394.6 K). These specimens also had larger periodicities. A specimen made with greater amounts of cross-linking agent (111 phr) possessed higher T_gs, ranging from 130 °C (403 K) to 143 °C (416 K). A comparison between the periodicity of the BLT and the glass transition temperature is shown in

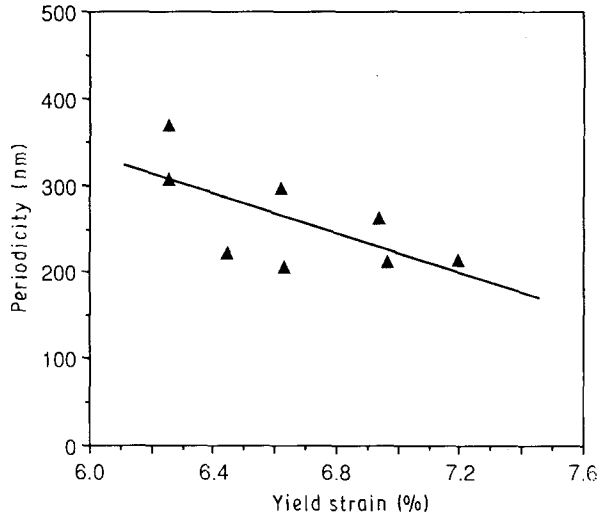

Figure 12 Comparison between the periodicity of the basic longitudinal texture and the yield strain.

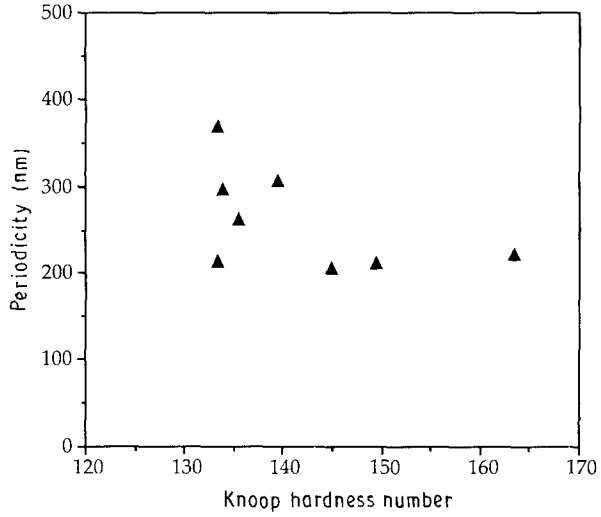

Figure 13 Comparison between the periodicity of the basic longitudinal texture and the hardness as measured by the Knoop hardness number.

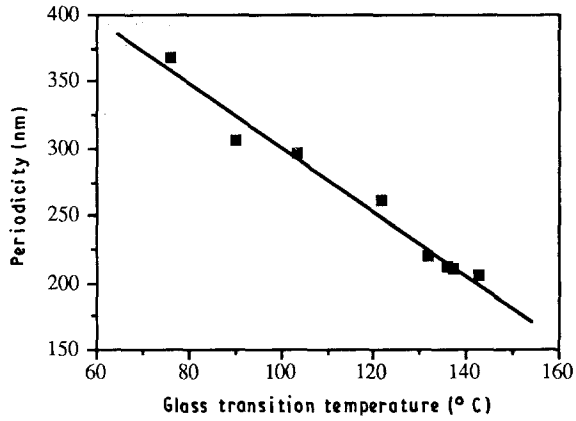

Figure 14 Comparison between the periodicity of the basic longitudinal texture and the glass transition temperature.

Fig. 14. The periodicity is seen to decrease nearly linearly with increasing T_g. The least square regression line through this data yields for the periodicity λ

$$\lambda(\text{nm}) = -2.36\,T_g(^\circ\text{C}) + 537 \qquad (2)$$

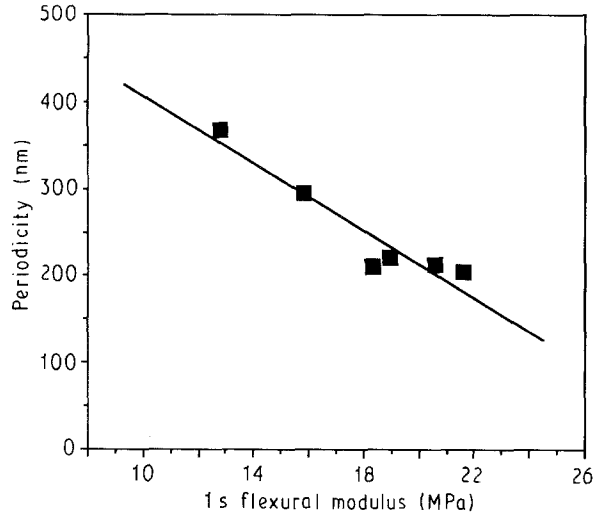

Figure 15 Comparison between the periodicity of the basic longitudinal texture and the 1 s modulus in the rubbery state at 200 °C.

The storage moduli of the epoxy specimens in the rubbery plateau region, $E_{R'}$, (the 1 s flexural moduli) were obtained from the DMA measurements. The moduli measured at 200 °C (a temperature much above the T_gs and well into the rubbery plateau region of all of the specimens) are listed in Table III. These moduli are seen to vary from 12.8 to 21.6 MPa. A comparison between the periodicity of the BLT and the 1 s moduli at 200 °C is given in Fig. 15. The periodicity is seen to decrease nearly linearly with increasing rubbery modulus. Statistical analysis by least square regression gives for the relationship between the periodicity and the modulus $E_{R'}$

$$\lambda(\text{nm}) = 599 - 19.3\, E_{R'}\,(\text{MPa}) \qquad (3)$$

4. Discussion

None of the mechanical properties of the solid state of the series of anhydride-cured epoxy specimens has been found to correlate significantly with the periodicity of the basic longitudinal texture. The mechanical properties examined were the Young's modulus, the non-linear pre-yield behaviour, the yield behaviour, both stress and strain at yield, and the hardness. It is only with the glass transition and the behaviour in the rubbery state above the glass transition that correlation with the periodicity of the basic longitudinal texture is found. Hence, the BLT seems to be related to the liquid properties above the T_g of the thermoset. These findings support the hypothesis mentioned earlier, that the BLT is the frozen remnant of the network glass having passed through the rubbery or liquid state during the fracturing process.

The glass transition temperature and the rubbery modulus both appear to be linearly related to the periodicity of the basic longitudinal texture. This is not too surprising since both are related to the crosslink density or the molecular weight between crosslinks. From the moduli in the rubbery plateau region, the average molecular weight of the network chains between crosslinks can be estimated by use of the statistical theory of rubber elasticity. According to this theory, the average molecular weight of the network chains, M_c, is given by

$$M_c = \frac{\rho RT}{G_{R'}} \qquad (4)$$

where ρ is the density (Mg m^{-3}), R the gas constant, T the absolute temperature, and $G_{R'}$ is the rubbery storage shear modulus ($G_{R'} = E_{R'}/3$) (MPa). Values for M_c computed from Equation 4 are given in Table II.

For the relationship between the glass transition temperature and the average molecular weight between crosslinks, Nielsen has derived the following empirical equation from data in the literature [13]

$$T_g - T_{g0} \approx \frac{3.9 \times 10^4}{M_c} \qquad (5)$$

where T_{g0} is the glass transition temperature of the uncrosslinked polymer having the same chemical composition as the crosslinked polymer. The glass transition temperature for the series of anhydride-cured epoxy specimens is plotted against $1000/M_c$ in Fig. 16 and a fair fit to a straight line is found. The slope of the line is 1.09×10^5, somewhat larger than the coefficient in Equation 5.

The linear relationships expressed in Equations 2 and 3 between the periodicity of the BLT and the glass transition temperature and the rubbery modulus suggest the occurrence of possibly non-physical intercepts. The periodicity is suggested by Equations 2 and 3 to vanish when $T_g = 227.5$ °C or when $E_{R'} = 31.0$ MPa and to become negative at larger values of these properties. Although these intercept values are specific for the anhydride-cured epoxy system studied, and might not be attainable experimentally, an exact linearity with the periodicity is doubtful. Although the fitting of all of the data of periodicity against T_g by a single straight line in Fig. 14 is statistically significant, a better fitting can be obtained by analysing separately the data for the two different amounts of anhydride curing agent. This is shown in Fig. 17. This fitting suggests that over

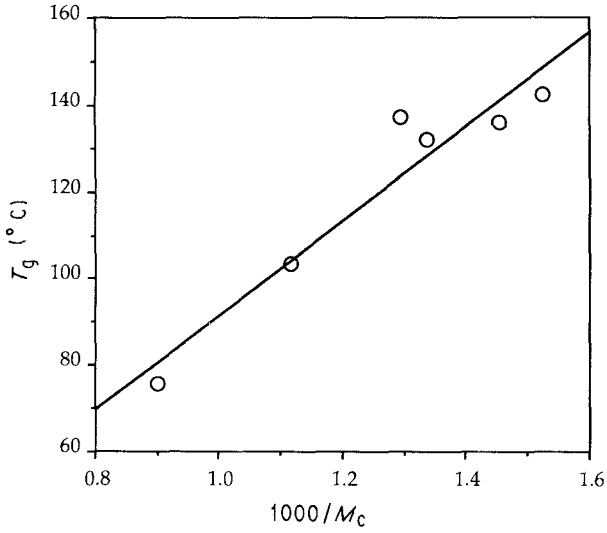

Figure 16 Comparison between the glass transition temperature and the reciprocal of the average molecular weight between the crosslinks.

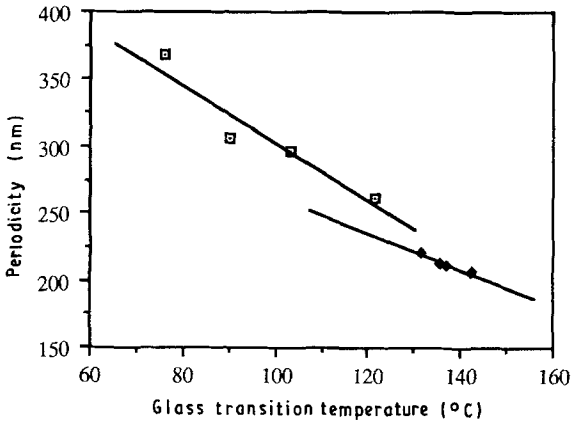

Figure 17 Comparison between the periodicity of the basic longitudinal texture and the glass transition temperature, analysing separately the 44 phr (□) and the 111 phr (◆) anhydride containing specimens.

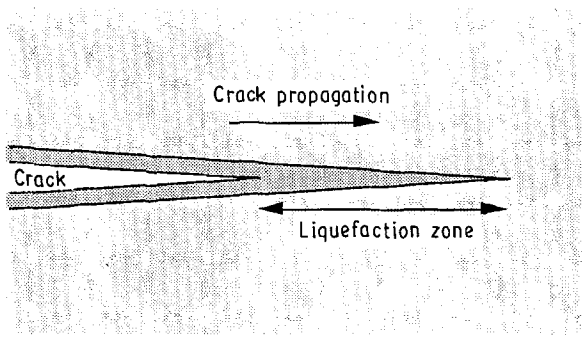

Figure 18 Schematic representation of the liquefaction zone suggested to be induced at the crack tip during the brittle fracture of network glasses. The remnant of liquefaction, the basic longitudinal texture, is shown as a thin boundary contiguous with both surfaces of the crack.

a broader range of glass transition temperatures, the relationship between λ and T_g becomes a concave-upward curve that either avoids an intersection with the abscissa (at $\lambda = 0$) or pushes the intersection out to very large values of T_g.

As was mentioned above, the findings of this work support the hypothesis that the BLT is the frozen remnant of the network glass having passed through the rubbery or liquid state during fracture. The sequence of events suggested are indicated in Fig. 18. Liquefaction is induced in the brittle solid by the stress field in front of the crack front. Ironically, it is across the resulting *liquid* layer that the actual separation of brittle fracture is suggested to occur. While the two pieces are separating, the unstable surface of the liquified network glass at the crack front evolves into the fingering pattern, which causes the basic longitudinal texture to develop.

How does the hypothesized liquefaction arise? It is possible for network polymers with low T_gs to liquify by heating. For example, Kambour and Barker [14] estimated that an increase in the temperature of as much as 212 °C could occur during the fracture of poly(methyl methacrylate), depending on the crack velocity. Hence, the heat generated by the fracturing process at room temperature could conceivably raise the temperature of PMMA far above its glass transition (105 °C). A similar conclusion was reached more recently by Swallowe *et al.* [15].

Liquefaction need not, however, result from an elevation in temperature. Indeed, the lack of significant difference in the periodicity from 60 to − 180 °C despite the large difference in the fracturing temperature indicates that the liquid state is not attained solely (or even mainly) by heating. (The periodicity of the specimen in Fig. 4a fractured close to − 180 °C was about 200 nm; that of the specimen in Fig. 4b fractured at 60 °C was about 250 nm.) Although the temperature of the material probably increases on fracturing, even to reach the glass transition temperatures of the epoxy specimens, which ranges from 76 to 142 °C, from − 180 °C would require temperature increases in the range of 250 to 340 °C. Moreover, of the total heat generated, only a fraction would be available for liquefaction. Much of the heat would be generated *after* the fluidity has increased sufficiently for the material to undergo large deformation.

Liquefaction is more likely to be induced by the intense stress field in a process similar to, if not identical to, yielding. This process is equivalent to the excitation of only one or several degrees of freedom, rather than of all of them as occurs during heating [16]. There have been two general approaches to understanding the mechanism of yielding. In one, the approach of Argon and Bessonov [17, 18], Robertson [19–21], and others, it is suggested that the liquefaction of yielding is induced by the shear component of the applied field, which reduces the stiffness of the polymer chain (e.g., by the "flexing" of bonds, as in Robertson's model). In the other approach, that of Newman and Strella [22], Matsuoka *et al.* [23–25], and others, it is suggested that the liquefaction is induced by hydrostatic tension, which increases the volume. The volume increases under application of hydrostatic tension because Poisson's ratio is less than one-half for polymer glasses and most other solids. Liquefaction arises from an increase in free volume, which is assumed to accompany, if not to equal, the increase in total volume.

After liquefaction by the intense stress field ahead of the crack, fingering develops at the crack front as described by Taylor [5], Argon and Salama [6], and Fields and Ashby [26]. The basic longitudinal texture probably develops from the fingering as follows. The fingers protruding ahead of the nominal crack front create the grooves in the BLT, and the membranes between the fingers create the ridges. The membranes, and the ridges that they become on breaking, are probably pulled out from the surface. The plasticity involved in this is not unlike that seen elsewhere in the fracturing process with brittle thermosets [8, 27]. The ridges are probably analogous to the fibrils of crazing (which seem to be prevented from occurring by the crosslinks). If the separated fracture surfaces were brought together again, ridges are expected to stand opposite to ridges and grooves opposite to grooves.

The permanent existence of the BLT seems to be a result of the rapid freezing of the surfaces and occurs when the stress field that caused the liquefaction is suddenly removed as the fracture surfaces separate.

The glass transition temperature, the elastic modulus of the rubbery state, and the average molecular weight between crosslinks are seen to be interrelated. From which does the periodicity of the BLT arise? The temperature span between the fracturing temperature and the glass transition is a measure of the energy needed for liquefaction, whether as heat or mechanical work. If the periodicity were a reflection of this energy, then for a fixed fracturing temperature, the glass transition temperature could be described as determining the magnitude of the periodicity. This would imply, however, that the periodicity would change as rapidly with change in fracturing temperature as it does with change in glass transition temperature, namely by 230 nm per 100 °C. When the fracturing temperature for a typical specimen was changed from around $-180°$ to $+60$ °C, however, the periodicity changed by 50 nm or less. The periodicity seems not to be determined solely by the energy required for liquefaction or by the glass transition temperature *per se*. Of the remaining two, the rubbery modulus and the crosslink density or molecular weight between crosslinks, each may be equally significant for the periodicity and simply be a different reflection of the same thing. The periodicity seems to depend on the modulus, but according to the details of the stress configuration at the crack front, the dependence may be on the shear modulus, G_R, the flexural or tensile modulus, E_R, or the bulk modulus, K_R [28, 29]. The latter, however, is expected to depend on the crosslink density but not on the shear or flexural modulus *per se*.

5. Conclusions

The results of this work suggest that the brittle fracture of polymer network glasses involves the liquefaction of the glass ahead of the crack front. The actual severing of the glass then involves the separation of the pieces across this liquid layer.

The property investigated in this study for a series of anhydride-cured epoxy specimens has been the basic longitudinal texture (BLT). This is the finest texture observed on fracture surfaces and consists of low ridges and shallow grooves that are aligned parallel with the direction of crack propagation. The periodicity of the BLT (the average lateral separation between adjacent ridges or grooves) has been found to be characteristic of each material. When compared with other properties of the material, only properties of the liquid state, namely, the glass transition temperature and the rubbery modulus, were found to correlate well with it. This suggests that the BLT is the remnant left on the fracture surfaces of a liquid state that must have developed during fracture, probably by the intense stress field associated with the crack front. The BLT is suggested to arise from a profusion of fingers in the crack front that extend ahead of the rest of the crack. These fingers are suggested to create the grooves in the BLT with the polymer stretched into membranes between. When the membranes break, they then form the ridges. The fingering is suggested to arise from the well known instability that develops in moving air–liquid interfaces [5].

Since the basic longitudinal texture has been found on the fracture surfaces of a borosilicate glass [4], the above may be characteristic of the brittle fracture of *all* network glasses, both organic and inorganic.

Acknowledgements

The authors are particularly grateful to Mr Michael Sporer and Ms Viorica Mindroiu for preparing the specimen and obtaining the micrograph in Fig. 3. We also wish to thank Dr Sandy Labana, Dr Henk Van Oene and Mr Mo-Fung Cheung (Ford Motor Co.) and Professor David C. Van Aken (University of Michigan) for allowing us to use their TMA and DMA instruments, respectively, and to Dow Chemical USA (Freeport) and Mrs Dorothy Babbington for providing the epoxy resin. This work was supported in part by the NSF Center for Advanced Cement-Based Materials, NSF Grant No. 0830-350-B600-UM-HA.

References

1. R. E. ROBERTSON, V. E. MINDROIU and M. F. CHEUNG, *Compos. Sci. Tech.* **22** (1985) 197.
2. R. E. ROBERTSON and V. E. MINDROIU, *J. Mater. Sci.* **20** (1985) 2801.
3. *Idem., Polym. Eng. Sci.* **27** (1987) 55.
4. T. Y. PAN, R. E. ROBERTSON and F. E. FILISKO, *J. Mater. Sci.* **24** (1989) 3635.
5. G. I. TAYLOR, *Proc. R. Soc. A* **201** (1950) 192.
6. A. S. ARGON and M. SALAMA, *Mater. Sci. Engng* **23** (1976) 219.
7. A. M. DONALD and E. J. KRAMER, *Phil Mag. A* **43** (1981) 857.
8. R. E. ROBERTSON, M. G. SPORER, T. Y. PAN and V. E. MINDROIU, *J. Mater. Sci.* **24** (1989) 4106.
9. G. G. TRANTINA, *J. Amer. Ceram. Soc.* **60** (1977) 338.
10. C. BULTEL, J. M. LEFEBVRE and B. ESCAIG, *Polymer* **24** (1983) 476.
11. J. M. LEFEBVRE, C. BULTEL and B. ESCAIG, *J. Mater. Sci.* **19** (1984) 2415.
12. G. COULON, J. M. LEFEBVRE and B. ESCAIG, *ibid.* **21** (1986) 2059.
13. L. E. NIELSEN, *J. Macromol. Sci., Rev. Macromol. Chem.* **C3** (1969) 69; "Mechanical Properties of Polymers and Composites", Vol. 1 (Marcel Dekker, New York, 1974) pp. 23–25.
14. R. P. KAMBOUR and R. E. BARKER, Jr., *J. Polym. Sci. A* **24** (1966) 359.
15. G. M. SWALLOWE, J. E. FIELD and L. A. HORN, *J. Mater. Sci.* **21** (1986) 4089.
16. R. E. ROBERTSON, to be published.
17. A. S. ARGON and M. I. BESSONOV, *Polym. Engng Sci.* **17** (1977) 174.
18. *Idem., Phil. Mag.* **35** (1977) 917.
19. R. E. ROBERTSON, *J. Chem. Phys.* **44** (1966) 3950.
20. *Idem., Appl. Polym. Sympos.* **7** (1968) 201.
21. R. P. KAMBOUR and R. E. ROBERTSON, "Mechanical Properties of Polymers", *Polymer Science*, edited by A. D. Jenkins (North-Holland, London, 1972) p. 688.
22. S. NEWMAN and S. STRELLA, *J. Appl. Polym. Sci.* **9** (1965) 2297.
23. S. MATSUOKA, C. J. ALOISIO and H. E. BAIR, *J. Appl. Phys.* **44** (1973) 4265.
24. S. MATSUOKA, H. E. BAIR, S. S. BEARDER, H. E. KERN and J. T. RYAN, *Polym. Engng Sci.* **18** (1978) 1073.

25. T. T. WANG and S. MATSUOKA, *J. Polym. Sci.: Polym. Lett. Edn* **18** (1980) 593.
26. R. J. FIELDS and M. F. ASHBY, *Phil. Mag.* **33** (1976) 33.
27. R. L. PATRICK, J. A. BROWN, N. M. CAMERON and W. G. GEHMAN, *Appl. Polym. Symp.* **16** (1971) 87.
28. J. S. COVAVISARUCH, PhD Thesis, The University of Michigan (1990).
29. J. S. COVAVISARUCH, F. E. FILISKO and R. ROBERTSON, to be published.

Received 17 October 1990
and accepted 25 March 1991